Available online at www.sciencedirect.com
ScienceDirect
Tetrahedron
Tetrahedron 63 (2007) 2391–2403

The dynamic covalent chemistry of mono- and bifunctional boroxoaromatics

Lyndsey M. Greig, Alexandra M. Z. Slawin, Melanja H. Smith and Douglas Philp*

EaStCHEM and Centre for Biomolecular Sciences, School of Chemistry, University of St Andrews, North Haugh, St Andrews, Fife KY16 9ST, United Kingdom

Received 29 June 2006; revised 7 December 2006; accepted 14 December 2006
Available online 17 December 2006

Abstract—10-Hydroxy-10,9-boroxophenanthrene reacts rapidly and reversibly with both benzylic and alkane diols in non-polar solvents. The formation of 2:1 adducts between the boroxoaromatic and the diols is favoured. The diol component of the adduct can be exchanged readily and rapidly by treatment of the boroxoaromatic–diol adduct with an alternative diol in solution at room temperature. This reversible covalent chemistry would appear to be ideal for the dynamic assembly of more complex superstructures. However, attempts to extend this dynamic equilibrium to the assembly of macrocycles using the bifunctional boroxoaromatic 5,9-dihydroxy-5,9-dibora-4,10-dioxopyrene failed as a result of changes in the reactivity of the boron centre in the bifunctional boron-containing compound.

1. Introduction

The construction[1] of large, regular superstructures in biological systems is usually accomplished through the application of self-assembly processes. Examples include the folding[2] of proteins, the stepwise assembly[3] of the tobacco mosaic virus and the self-regulated construction[4] of the virus T4 bacteriophage. Several key principles govern self-assembly processes: self-assembly processes are highly convergent and, thus economical in the amount of information required to encode the target structures. In general, self-assembling systems use a relatively small number of simple and often identical units to create functionally and structurally complex arrays. Therefore, self-assembling systems typically require only a small set of different interactions to create the final molecular assembly. The entire assembly process is a dynamic one in which all the assembly/disassembly steps are reversible. This reversibility is most often accomplished using weak non-covalent interactions. The result of this reversibility is a degree of error checking. Incorporation of an incorrect subunit results in an increase in free energy and is not tolerated. These spurious additions to the structure are reversed in a drive to minimize the total free energy of the system. Given these advantages, it is desirable for chemists to mimic self-assembling systems of this kind. Indeed, considerable effort has been directed towards the formation[5] of synthetic supramolecular self-assembled architectures in which the assembly process is directed by selective interactions, for example, hydrogen bonds[6] or metal–ligand[7] coordination. There is, however, one major disadvantage to the use of non-covalent interactions in synthetic self-assembling systems. On formation of the superstructure, a large and unfavourable change in entropy arises from the ordering of the components. The formation of non-covalent bonds affords only a small amount of enthalpic stabilization per interaction and, therefore, a significant number of these interactions is required before this stabilization offsets the entropic loss.

One answer to this problem lies in the use of covalent bonds as a means of constructing large regular assemblies. Covalent bonds are stronger than hydrogen bonds and, hence, a smaller number is required to produce a stable assembly. Traditionally, covalently linked structures have been synthesized using sequential, kinetically controlled, and irreversible reactions. However, the linear formation of such large structures requires a high number of synthetic steps and is extremely time consuming. To date, the use of covalent interactions in the field of self-assembly has been relatively under-exploited. The use of covalent bond formation[8] in self-assembly processes requires that these bonds form under thermodynamic control, i.e., bond formation is reversible, as, for example, in the cases of disulfides[9] or borate[10] esters. An example of a system that employs covalent bonds in a thermodynamically controlled assembly process has been described by Sanders and co-workers.[11] The cyclization of the cinchonidine monomer, methyl-10,11-dihydroquinine-11-carboxylate, might be expected[12] to generate

Keywords: Self-assembly; Molecular recognition; Aromatic compounds; Dynamic covalent chemistry; Reversible reactions.
* Corresponding author. Tel.: +44 1334 467264; fax: +44 1334 463808; e-mail: d.philp@st-andrews.ac.uk

0040–4020/$ - see front matter © 2006 Elsevier Ltd. All rights reserved.
doi:10.1016/j.tet.2006.12.034

a wide range of oligomers. However, in practice, the trimer is found to be the most stable product. The preference to form the trimer is not a result of preorganization within the monomer, but rather a result[13] of predisposition. Ipaktschi and coworkers[14] have also exploited reversible covalent bond formation in a self-assembled synthetic strategy. The ultimate expression of the power of dynamic covalent chemistry for the assembly of complex superstructures is described in the synthesis of Borromean rings by Stoddart and coworkers.[15] In this system, a complex set of interlocked macrocycles is created in a single step by metal-directed dynamic imine chemistry. The field of dynamic covalent chemistry is hampered, however, by the relatively small group[16] of reactions that are truly reversible under conditions that are compatible with a wide range of functional groups.

We have described[17] the assembly of a dimeric macrocycle through the exploitation of a novel class of compounds—borazaaromatics. When the monomer **1** is dissolved in acetone solution, the compound reacts with itself to form a dimeric macrocycle **2** by exploiting reversible homoanhydride formation. Although the reversible chemistry[18] provided by borazaaromatics is attractive building blocks for use in covalent self-assembly processes, the spontaneous formation of homoanhydrides limits their application[19] in this context by making the incorporation of structurally diverse subunits difficult. Additionally, their low reactivity towards other nucleophiles limits the complexity of structures that can be assembled using these building blocks. Through the model compound **3**, we have demonstrated[20] that the corresponding oxygen-containing boroxoaromatics are suitable compounds to extend the use of boron-containing heteroaromatics in covalent self-assembly processes. In solution, they do not form homoanhydrides, but do form mixed esters with alcohols reversibly and rapidly, even at low (<-40 °C) temperatures.

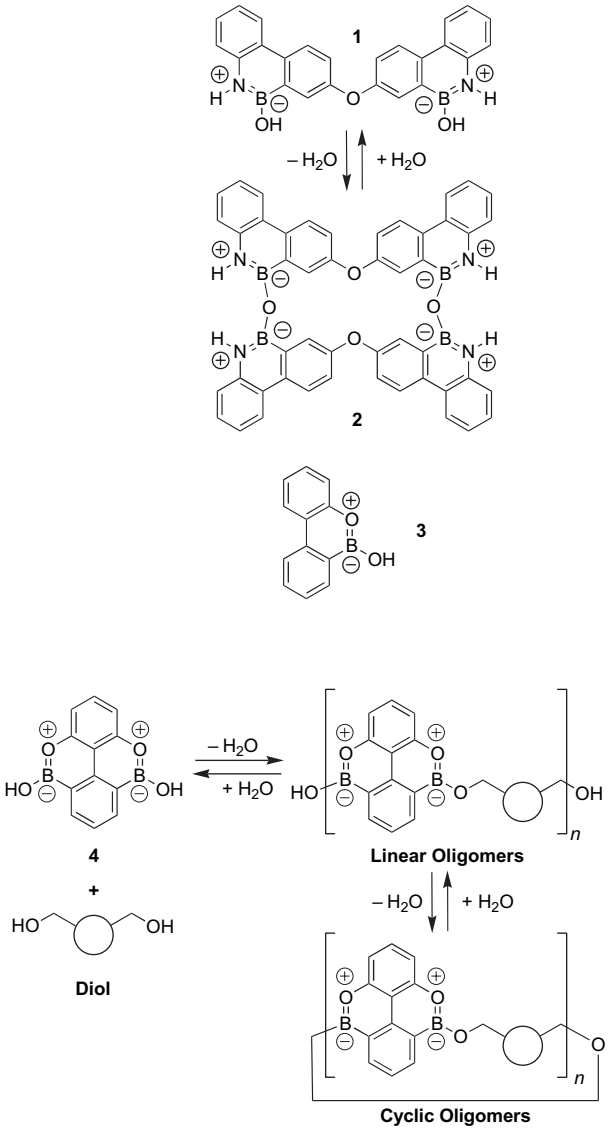

Figure 1. Bis-boroxoaromatic **4** may react with a diol in solution to form linear oligomers and/or cyclic oligomers reversibly.

Here, we describe the design and synthesis of a bifunctional boroxoaromatic and its behaviour in both solution and solid states and attempts to exploit its solution phase properties in dynamic assembly processes.

Drawing from our previous work on bis-borazaaromatics we identified the bis-boroxoaromatic **4** as a suitable synthetic target. We envisaged that this compound could react (Fig. 1) with a series of mono-, di-, and triols to give a range of self-assembled structures. Based on a rigid pyrene skeleton, compound **4** should react rapidly and reversibly with nucleophiles such as alcohols in a similar fashion to that observed for **3**. It should be possible to monitor the formation of linear hetero-oligomers **5** in solution (Fig. 1). The reaction between **4** and a nucleophile in solution would be under thermodynamic control and should give the most stable product that may be macrocyclic or polymeric.

2. Synthesis

Compound **4** can be accessed readily from the precursor diphenol **5** (Scheme 1), which in turn can be constructed by applying standard metal-catalyzed cross-coupling methodology[21] to an appropriately protected 2,6-dihydroxyhalogenobenzene.

Addition[22] (Scheme 1) of sodium hydrogen carbonate to an equimolar mixture of 1,3-dihydroxybenzene **6** and iodine in water resulted in the precipitation of 2,4,6-triiodoresorcinol, which was removed by filtration. Work-up of the filtrate afforded 2-iodoresorcinol **7**. Protection of the phenolic groups as their benzyl ethers followed by metal-catalyzed cross-coupling using either Kharasch or Suzuki methodology afforded the benzyl-protected 2,6-dihydroxybiphenyl **9**. Deprotection of the benzyl ethers using standard methodology afforded the target phenol **5**. An alternative and shorter synthesis was also employed. Treatment[23] of 1,3-dimethoxybenzene **10** with *t*-BuLi led to selective deprotonation of the 2-position of the aromatic ring, and reaction with iodine gave 2,6-dimethoxyiodobenzene **11** in moderate yield. The yield of the subsequent Ni-catalyzed Kharasch cross-coupling with PhMgBr was found to vary greatly with the identity of the catalyst. With [Ni(dppe)Cl_2], the desired 2,6-dimethoxybiphenyl **12** was obtained only in low yield (18%), with the homocoupling product, biphenyl, accounting

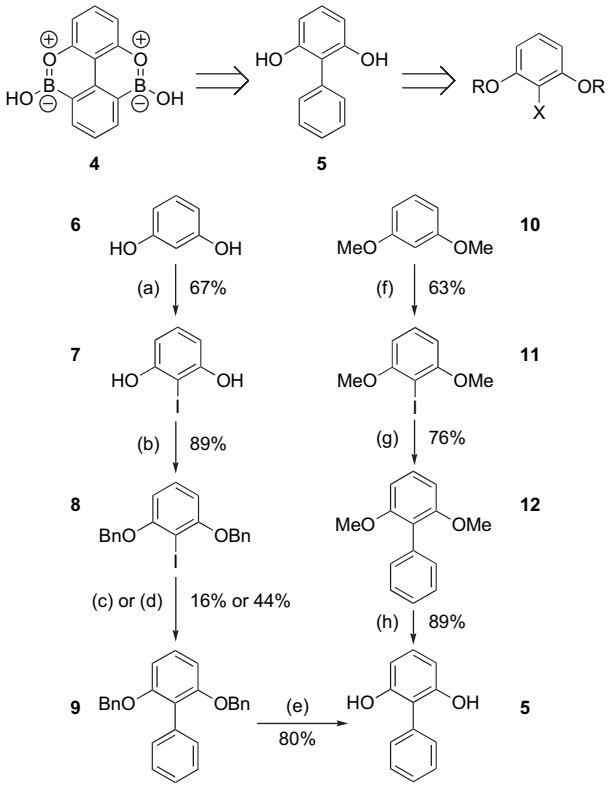

Scheme 1. Reagents and conditions: (a) I_2, $NaHCO_3$, H_2O; (b) $PhCH_2Br$, K_2CO_3, 18-C-6, Me_2CO; (c) $PhB(OH)_2$, $Pd(PPh_3)_4$, Na_2CO_3, DME, EtOH, H_2O, 18 h; (d) PhMgBr, $[Ni(dppe)Cl_2]$, Et_2O, 18 h; (e) Pd/C, H_2, MeOH, rt; (f) *t*-BuLi, THF, 0 °C, I_2, THF; (g) PhMgBr, $[Ni(PPh_3)_2Cl_2]$, Et_2O, Δ and (h) BBr_3, CH_2Cl_2.

for the majority of the recovered material. The yield was significantly improved (78%) on changing the catalyst to $[Ni(PPh_3)_2Cl_2]$, and, furthermore, this method used only 2 mol % catalyst, rather than the 10 mol % required previously. The coupling was also attempted using Stille and Suzuki methodology, but neither resulted in an improved yield. Deprotection of **12** using BBr_3 gave the diphenol **5** in a 43% overall yield starting from **10**.

The cyclization of **5** to afford the target 5,9-dibora-4,10-dioxapyrene **4** proved problematic. In all, three different approaches were employed. When the same conditions utilized in the synthesis of boroxophenanthrene **3**, i.e., reaction of **5** with BCl_3, and subsequent cyclization with $AlCl_3$, only starting material was recovered. Reaction of **5** with BCl_3 results in the evolution of HCl, and it is possible that the initial O–BCl_2 adduct is not stable under the increasingly acidic reaction conditions. With this in mind, we employed $BHCl_2\cdot Me_2S$ as the boron source, hoping that this would solve this problem, however, once again, only starting material was recovered from the mixture. It is possible to follow the reaction of **5** with $BHCl_2$ by measuring the volume of H_2 gas produced during the process. In all cases, the volume of gas was found to be consistent with the volume expected for the formation of the intermediate oxoborondichloride adduct. Calculations have shown that the boron–oxygen bond is somewhat weaker than the boron–nitrogen bond in borazaaromatics. It may be that the oxoborondichloride adduct is simply too fragile to withstand the reaction conditions, and the O–B bond is cleaved before the cyclization has taken place.

A third method (Scheme 2) employed uncomplexed $BHCl_2$ as the boron source. $BHCl_2$ may be generated in situ by exploiting the greater Lewis acidity of BCl_3. Reaction of $BHCl_2\cdot Me_2S$ with BCl_3 in toluene results in the release of $BHCl_2$ from its complex as the Me_2S associates preferentially with the stronger Lewis acid and, under the conditions employed, the $BCl_3\cdot Me_2S$ complex precipitates from solution. The solution of $BHCl_2$ was then transferred by a syringe and used to treat a solution of **5** in toluene at room temperature. Formation of the intermediate adduct was monitored by the formation of H_2 gas. Once adduct formation was complete, the addition of $AlCl_3$ and heating effected cyclization to give the target compound in good yield.

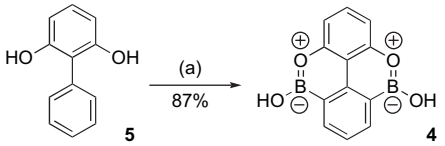

Scheme 2. Reagents and conditions: (a) (i) $BHCl_2$, PhMe and (ii) $AlCl_3$, PhMe, Δ.

In solution, the O–H bond vectors in **4** can adopt a variety of conformations with respect to the B–O bond, we label these conformations *anti–anti*, *syn–anti* and *syn–syn* (Fig. 2). The singlet resonance at δ 8.45 arises from the exchangeable hydroxyl proton H^e, since this signal disappears slowly when a drop of D_2O is added to the NMR sample. By comparison with the resonances observed in the ^1H NMR spectra of the precursors to **4**, we assign the doublet at δ 8.39, just upfield of the resonance arising from H^e to H^c. The other resonances

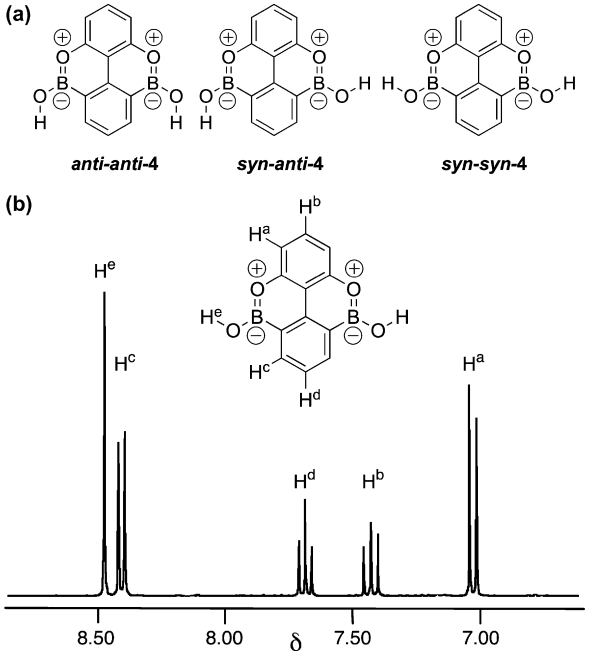

Figure 2. (a) The possible conformations of the O–H bond with respect to the B–O bond in **4**. (b) Partial 300 MHz ^1H NMR spectrum of **4**, recorded at 293 K in d_6-acetone. The resonance arising from H^e is assigned on the basis of its disappearance on addition of D_2O. The remaining four resonances can be tentatively assigned by COSY analysis.

are then readily assigned (Fig. 2) by COSY experiments. ^{1}H NMR spectroscopic analysis in d_6-acetone shows the bis-hydroxy monomer **4** only, as expected by analogy with **3**. Unfortunately, compound **4** is not soluble in $CDCl_3$, therefore we cannot determine with absolute certainty whether **4** is capable of reacting with itself in non-polar solvents. Some evidence for the preference of the *syn–syn* conformation comes from the lack of any observable NOE between protons H^e and H^c. Although H^e is, in principle, exchangeable, we have, in the past, been able to detect NOEs to and from this type of proton as their exchange rates are very slow. From this observation it is evident that the hydroxyl group adopts a *syn* conformation with respect to the boron–oxygen bond, rather than an *anti* conformation (in which an NOE effect would be observed, as, for example, in the case of **1**).

3. Electronic structure calculations

In order to compare the structural and electronic properties of **4** with the mono-functional compound **3** we carried out electronic structure calculations at the HF/6-31G(d,p) level of theory. Selected bond lengths and Löwdin bond orders in **4** and, for ease of comparison, **3** are shown in Table 1. It would appear that the incorporation of the second boroxoaromatic ring in **4** has little or no structural effect when the data are compared with that for compound **3**. The calculated structure is planar, and both O–H bond vectors are *syn* with respect to the endocyclic B–O bond. At this level of theory, *syn–syn*-**4** is around 30 kJ mol^{-1} more stable than *anti–anti*-**4**.

As in **3**, the hybridization of the exocyclic oxygen is confirmed to be closer to sp^2 than sp^3 by the C–B–O_{exo} and O_{endo}–B–O_{exo} bond angles (123° and 118°, respectively), and the calculated bond orders predict considerable π-character for both the endocyclic and exocyclic O–B bonds.

Table 1. Selected bond lengths and Löwdin bond orders in the calculated (HF/6-31G(d,p)) structures of **4** and **3**

Compound	Bond	Length/Å	Bond order
3	Endocyclic O–B	1.37	1.32
	Exocyclic O–B	1.35	1.45
	C–endocyclic O	1.35	1.17
	C–B	1.55	1.04
syn,*syn*-**4**	Endocyclic O–B	1.37	1.30
	Exocyclic O–B	1.35	1.45
	C-endocyclic O	1.35	1.18
	C–B	1.55	1.04

4. Solid state structure

Single crystals of **4**, suitable for analysis[24] and structure determination by X-ray diffraction, were grown by slow evaporation of a solution of **4** in acetonitrile. Compound **4** crystallizes in the space group $I4_1/a$. The packing of **4** (Fig. 3a) is dominated by cyclic arrays (**A** and **B**) of four O–H···O hydrogen bonds between hydroxyl groups attached to the boron atoms of **4**. Interestingly, these cyclic arrays propagate in different ways through the structure. In array **A**, the hydrogen bonds are between four molecules of **4** at the same level in the stack—the array is discrete. By contrast, array **B** is helical and extends continuously along the *c* direction of the crystal. This difference in propagation has a dramatic effect on the hydrogen bonding distances in the two arrays. In array **A**, the hydrogen bonds are significantly shorter (O–H···O distance=1.867 Å; O–H···O angle=160.3°; O···O distance=2.809 Å) than those present in array **B** (O–H···O distance=1.898 Å; O–H···O angle=172.0°; O···O distance=2.869 Å). This difference may reflect more effective polarization of the hydrogen bond donor atoms in the cyclic array as compared to the extended array. Each molecule of **4** is associated with one array of type **A** and one array of type **B** and the **A** and **B** arrays are related by translation in the *a* and *b* directions. Additionally, molecules of **4** are engaged in offset aromatic stacks along the *c* direction.

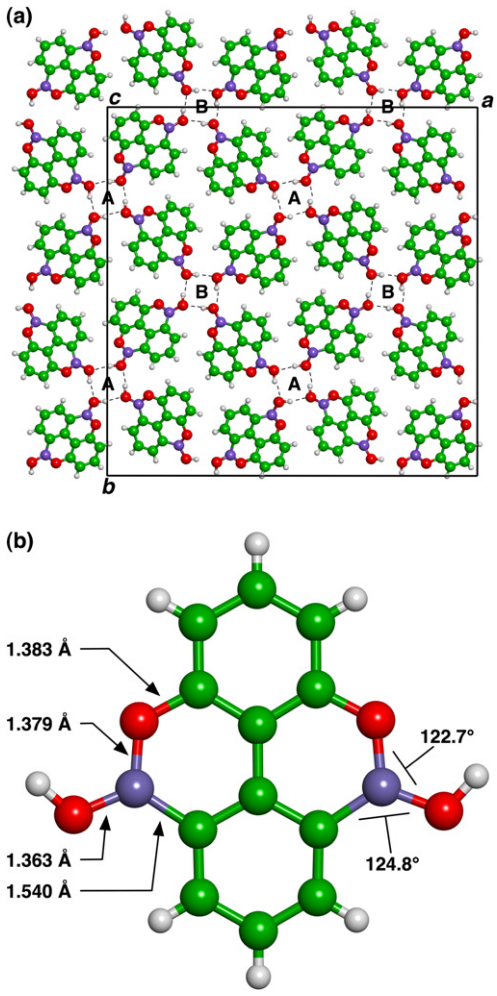

Figure 3. (a) Packing of compound **4** in the solid state. Hydrogen bonds are shown as dashed lines and the outline of the unit cell is shown as a solid line. (b) Molecular structure of compound **4** determined by single crystal X-ray diffraction. Carbon atoms are coloured green, boron atoms are mauve, oxygen atoms are red and hydrogen atoms are light grey.

The molecular structure of **4** in the solid state determined by X-ray diffraction (Fig. 3b) is in close agreement with that calculated (Table 1) using electronic structure methods.

5. Solid state reactivity

The solid state structure of **4** revealed that the hydroxyl groups in one molecule of **4** with a boron atom in the

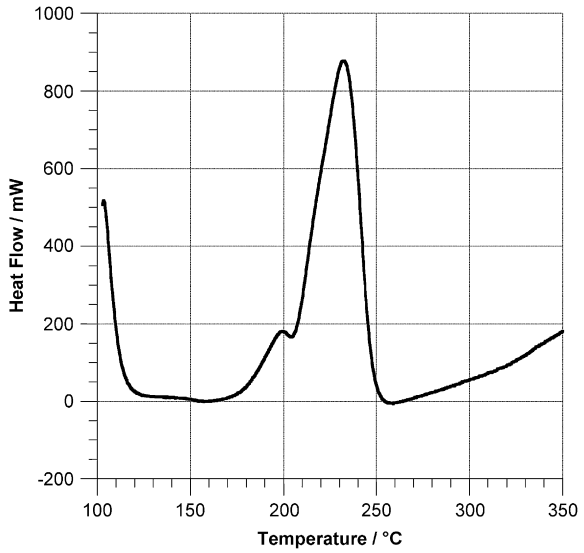

Figure 4. DSC trace recorded on heating a sample of **4** from 100 to 350 °C, at 50 °C min^{-1}. The onset of the solid state dehydration of the sample is clearly visible at 220 °C.

molecule of **4** in the layer above are in relatively close proximity (<4.5 Å). This observation suggested that reaction among molecules of **4** may well occur in the solid state. We therefore investigated the behaviour of **4** in the solid state by thermal analysis and powder X-ray diffraction.

Samples of **4** do not melt below 400 °C, which is suggestive of polymerization[25] occurring in the solid state. Initially, the solid state reactivity of **4** was investigated (Fig. 4) using differential scanning calorimetry (DSC). When heated to 350 °C at a rate of 50 °C min^{-1}, an endotherm is observed with an onset temperature of 220 °C. When the sample is subsequently cooled at the same rate, no exotherm is observed. Therefore, this endotherm is clearly not a result of the sample melting, and therefore suggests a phase change, perhaps as a result of a chemical reaction. The DSC analysis also exhibits a second small endotherm with an onset temperature of around 175 °C. The origins of this event have, so far, not been identified, but it may be a consequence of reorganization within solid state structure prior to reaction.

The powder X-ray diffraction pattern of **4** at room temperature is shown in Figure 5a and is in close agreement with the pattern predicted on the basis of the single crystal X-ray analysis. In order to probe the change in the solid state structure of **4** that occurs on heating, we employed variable temperature powder X-ray diffraction experiments. As the sample was heated to 300 °C, the reflections gradually became less intense. However, even after heating for 3 h, the sample does not appear to be completely amorphous (Fig. 5b). Clearly a major structural change is occurring within the sample.

In order to probe this change further, we decided to probe for a chemical change by employing thermogravimetric analysis. If the sample of **4** was converted to the oligo(anhydride) **13** under heating, we would expect water to be evolved and, at temperatures above 100 °C, it would be lost from the sample. We would therefore expect that the sample mass would decrease. In fact, complete conversion of **4** to

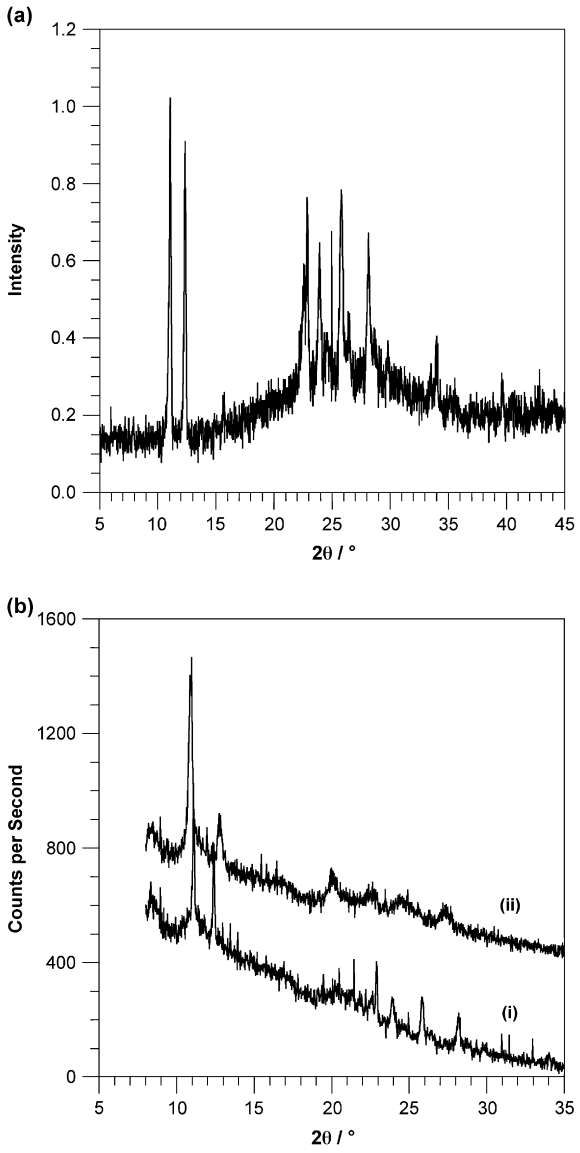

Figure 5. (a) Powder X-ray diffraction pattern for a sample of **4**, recorded at room temperature. (b) Powder X-ray diffraction patterns recorded (i) at 30 °C, for a sample of **4**, and (ii) after heating a sample of **4** at 300 °C for 180 min.

the poly(anhydride) would result in a mass loss of 7.6% of the total. Initially, a small sample (typically 3 mg) of **4** was heated from 30 to 300 °C at a rate of 50 °C min^{-1}. At this rate, a slight loss of mass from the sample is visibly evident at temperatures around 75 °C, and above (Fig. 6a). At about 200 °C, the rate of mass loss is noticeably increased, until a total mass loss of around 8% has occurred. After this point, a further slower mass loss is recorded, possibly as a result of sublimation or decomposition of the sample at the highest temperatures employed in the experiment. It is important to note that the mass loss observed by TGA is synchronous with the endotherm recorded by DSC. In order to study the mass loss more accurately, a sample of **4** was heated rapidly (100 °C min^{-1}) to 200 °C, in order to minimize any mass loss prior to the subsequent isothermal stage (Fig. 6b). The sample was then held at 200 °C for 10 min and a mass loss of around 8% was again observed, which is consistent with the formation of the poly(anhydride) **13**.

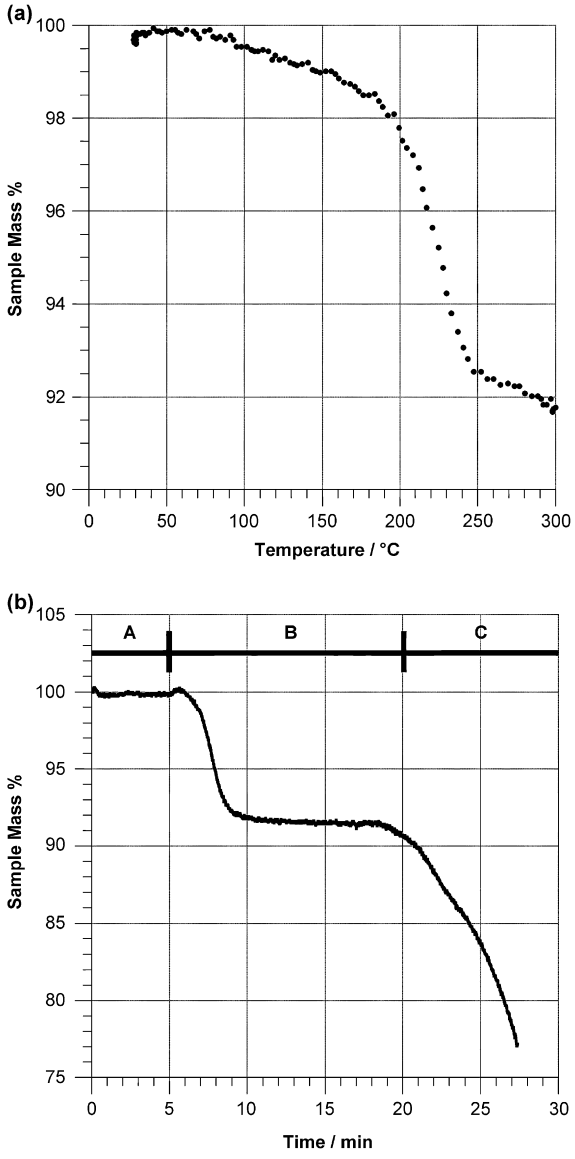

Figure 6. (a) Heating a sample of **4** from 30 to 300 °C results in continuous mass loss above 75 °C. The results shown were recorded over a period of around 10 min. One in every 30 data points are shown. (b) Thermogravimetric analysis of a sample of **4**. Region **A**: held at 30 °C for 5 min before heating to 200 °C at a rate of 100 °C min^{-1}. Region **B**: isothermal at 200 °C for 15 min resulting in a mass loss of around 8%. Region **C**: continued heating to 700 °C at a rate of 50 °C min^{-1}.

Continued heating from 200 to 700 °C, leads only to a further mass loss, due to sample decomposition.

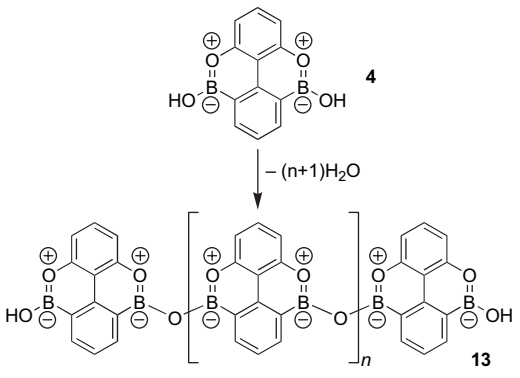

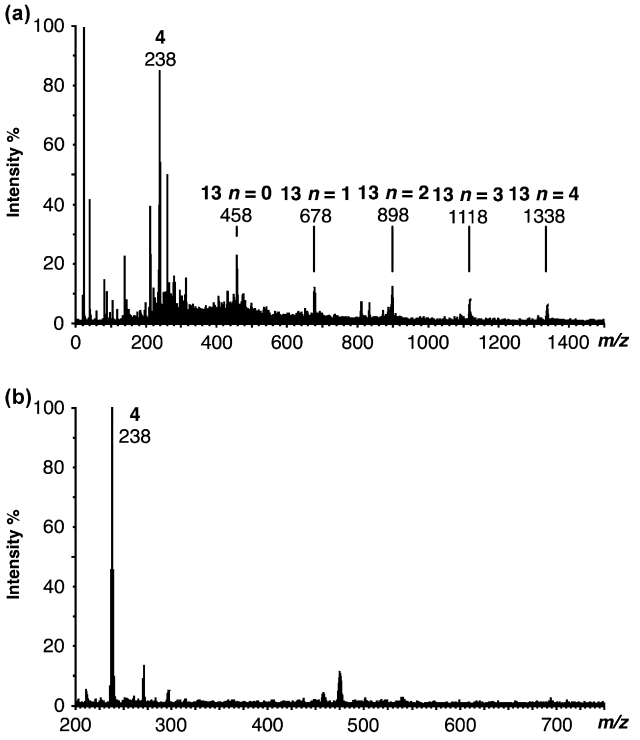

Figure 7. (a) MALDI-TOF mass spectrum for a sample of **4** recorded after heating at 200 °C for 10 min. The spectrum shows oligomers **4** up to the hexamer (n=4). (b) MALDI-TOF mass spectrum of a sample of **4**, which had not been heated above 30 °C.

In order to confirm the formation of the poly(anhydride) **13**, the sample was analyzed by MALDI-TOF spectrometry. It was necessary to dissolve the sample in acetone prior to application to the MALDI sample plate. Therefore, in order to minimize hydrolysis of any higher oligomers present in the sample, the acetone was pre-dried over 4 Å molecular sieves. MALDI-TOF mass spectral analysis of the sample resulting from the isothermal heating confirms the formation of oligomers up to the hexamer (Fig. 7, n=4). Although the most intense peak is due to the monomer **4**, it should be noted that MALDI spectrometry does not provide any quantitative measurement of the proportions of oligomers present.

For comparison purposes, the MALDI-TOF mass spectrum of a sample of **4** dissolved in acetone (Fig. 6b), recorded prior to heating under the conditions described above, shows that the monomer (m/z 238) is the dominant species present in this sample. We are therefore certain that the higher oligomers observed in Figure 7 are representative of the sample composition and this distribution of compounds is a result of sample heating and not the result of dehydration occurring during the recording of the spectrum.

6. Solution phase reactivity

We have demonstrated that 10-hydroxy-10,9-boroxophenanthrene is capable of reacting with oxygen nucleophiles, such as alcohols with loss of water to form covalent adducts, which retain the boroxoaromatic ring. We were therefore interested to explore the solution phase formation of oligomers by compound **4**. Potentially, reaction with bifunctional

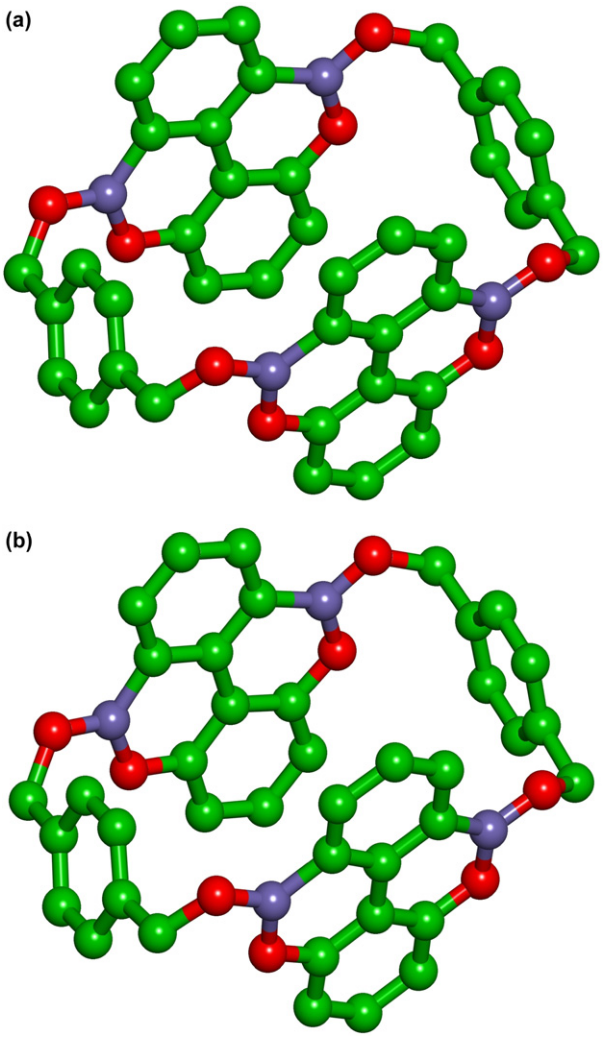

Figure 8. Calculated (AM1) structures of the 2+2 macrocycles formed from the reaction between: (a) **4** and **14**, and (b) **4** and **15**.

nucleophiles, such as benzenedimethanols **14** and **15**, could result in the formation of linear hetero(oligomers), of the type illustrated in Figure 1. However, semi-empirical electronic structure calculations suggested that macrocyclic structures were also accessible, with the 2+2 macrocycles being the most stable structures. Semi-empirical electronic structure calculations, using the AM1 method, reveal that both the macrocycle formed from two molecules of **4** and two molecules of 1,3-benzenedimethanol **14** (Fig. 8a) and that formed from two molecules of **4** and two molecules of 1,4-benzenedimethanol **15** (Fig. 8b) are relatively strain free.

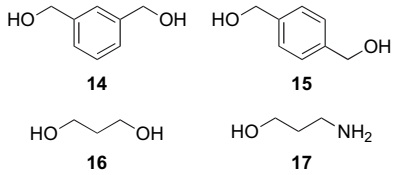

In order to test these possibilities, equimolar solutions of **4** with a series of nucleophiles, **14**, **15**, **16** and **17**, were prepared, and analyzed by ^{1}H and ^{11}B NMR spectroscopies and MALDI-TOF mass spectrometry. Since **4** is relatively

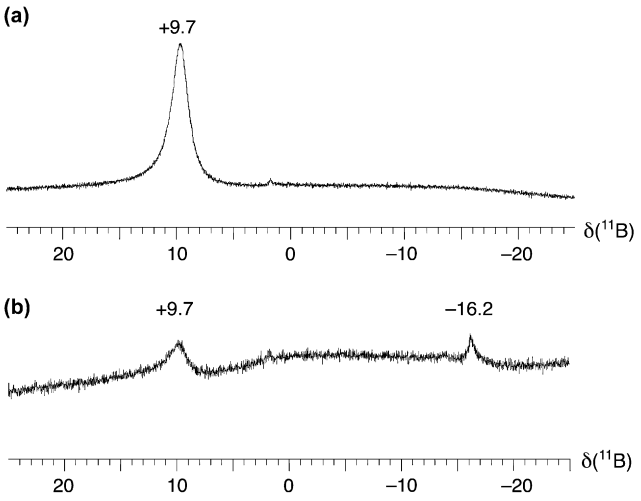

Figure 9. (a) The 160.4 MHz ^{11}B NMR spectrum of **4** recorded at 293 K in d_6-acetone. (b) The 160.4 MHz ^{11}B spectrum of a 1:1 solution of **4** and **17** in d_6-acetone. Both spectra were recorded using $B(OMe)_3$ in d_6-acetone as an external reference (δ=0.0). The poor signal-to-noise ratio in (b) is a result of the poor solubility of the adduct formed by **4** and **17** in d_6-acetone.

insoluble in solvents such as chloroform and acetonitrile, these experiments were performed in d_6-acetone. The solvent used in these experiments was dried thoroughly over anhydrous $CaSO_4$ prior to use and samples were left for a period of 24 h in the presence of anhydrous $CaSO_4$ prior to analysis. Disappointingly, in the cases of the reaction between **4** and **14**, **15** and **16**, 300 MHz ^{1}H NMR spectra, recorded in d_6-acetone showed only resonances characteristic of the unreacted starting materials. In the case of the reaction between **4** and **17**, ^{11}B NMR spectroscopy indicated that there were significant differences (Fig. 9) between the starting material **4** and the product of the reaction between **4** and **17**.

Whilst the ^{11}B NMR spectrum of **4** shows only a single resonance at δ +9.7, the addition of **17** to the solution results in the appearance of a second signal much further upfield at δ −16.2. The large upfield shift of the ^{11}B resonance suggests that the boron centre has undergone rehybridization from trigonal (sp^2) to tetrahedral (sp^3). It therefore seems likely that the second resonance arises from the formation of a structure such as **18** or **19**.

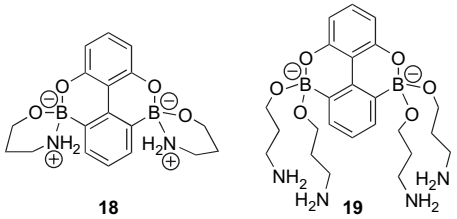

Analysis of the sample by MALDI-TOF mass spectrometry confirmed the identity of the new adduct as **18**—signals are observed at *m/z* 352 and 294 corresponding to the molecular ion of **18** and the corresponding monoadduct incorporating **4** and one molecule of **17**. The limited ability of **4** to form adducts with alcohols and other species was troubling given the ability of the corresponding monofunctional boroxoaromatic **3** to react readily with benzylic alcohols. In order to

assess whether this lack of reactivity was a result of an inappropriate choice of nucleophile or whether it was a property of compound **4** itself, we repeated the experiments described above using the monofunctional boroxoaromatic **3** in place of compound **4**. The results of these experiments are revealing. Boroxoaromatic **3** reacts rapidly and selectively with the benzenedimethanols **14** and **15** in d_6-acetone to form the 2:1 adducts **20** and **21**, respectively, which were characterized by ^{1}H and ^{11}B NMR spectroscopies and MALDI-TOF mass spectrometry. The exclusive observation of a signal at *m/z* 494 in solutions where there is an excess of **3** indicates that the 2:1 adduct is by far the dominant species. The 2:1 adducts **20** and **21** have ^{11}B chemical shifts of δ +9.0 and δ +9.6, respectively, indicating that the boron centre is still trigonal in these compounds.

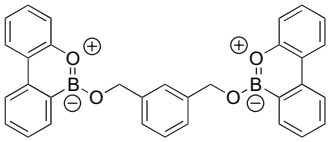

20

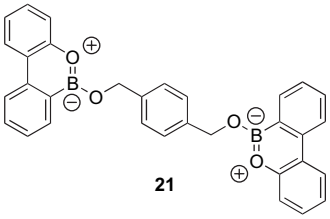

21

The more flexible propane-1,3-diol **16** can also form either a 1:1 or a 2:1 adduct with boroxoaromatic **3**. In this case, however, the 1:1 adduct can be stabilized by the interaction of the second OH group with the boron centre resulting in a six-membered chelate ring at boron and rehybridization of this centre to a tetrahedral (sp^3) geometry. Boroxoaromatic **3** reacts rapidly with propane-1,3-diol **16** in d_6-acetone to form the corresponding 2:1 adduct **22**. Characterization by MALDI-TOF mass spectrometry suggested that only the 2:1 adduct was present in the sample—a signal corresponding to adduct **22** was observed at *m/z* 432 whereas no signal was observed at *m/z* 254 corresponding to the 1:1 adduct **23**. ^{11}B NMR spectroscopy did, however, suggest that the 1:1 adduct **23** was present in solution—in addition to the resonance expected for the 2:1 adduct at δ +9.0 (sp^2 boron), an additional resonance at δ −0.4 was observed, indicating that a boron species was present in solution, which had undergone some rehybridization at boron, as would be expected for the 1:1 adduct **23**.

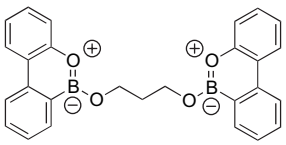

22

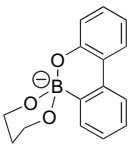

23

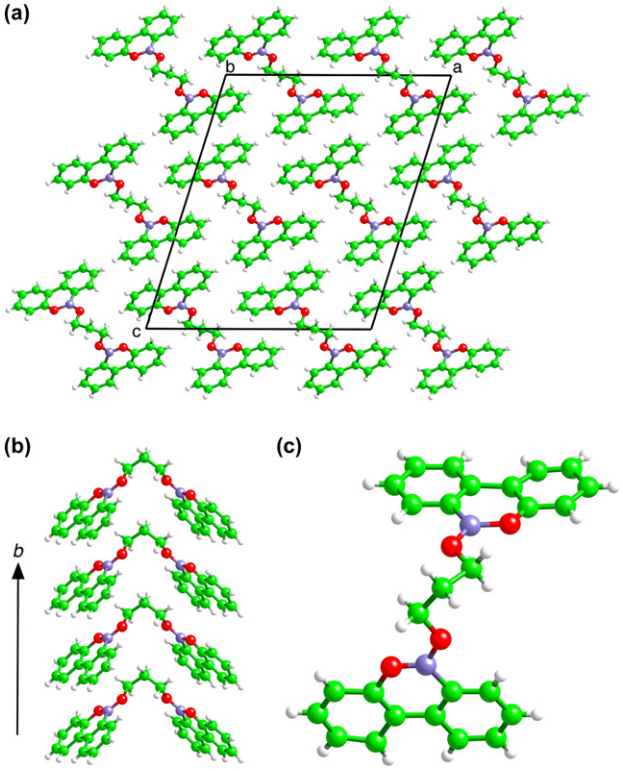

Figure 10. (a) Packing of compound **22** in the solid state. The outline of the unit cell is shown as a solid line. (b) Packing of compound **22** along the *b* axis in the solid state. (c) Molecular structure of compound **22** determined by single crystal X-ray diffraction. Carbon atoms are coloured green, boron atoms are mauve, oxygen atoms are red and hydrogen atoms are light grey.

Slow evaporation of a solution of **4** and **16** in d_6-acetone gave single crystals suitable for analysis[26] by X-ray diffraction. Structures revealed that these crystals were of the 2:1 adduct **22**. In the solid state, compound **22** is packed (Fig. 10a) in a series of paired stacks, which are related by translation in the *a* and *c* directions. In these pairs of stacks, the molecules of **22** adopt a conformation (Fig. 10b) in which the two aromatic planes are essentially at right angle to each other. The molecules stack along the *b* direction with the direction of adjacent stacks being opposite in sense giving rise to the pairing. It is noteworthy that within the molecular structure (Fig. 10c) of **22**, the *syn* arrangement of the exocyclic bond—in this case the C–O bond—with respect to the endocyclic B=O bond in the boroxoaromatic ring is observed strictly, even although this requires the linking of the trimethylene spacer to adopt a *gauche–gauche* conformation.

We have described previously dynamic exchange in esters of boroxoaromatic **3**. This dynamic behaviour is also present in compound **22**. When compound **22** is dissolved in d_6-acetone at room temperature and 1 equiv of 1,2-ethanediol and 1 equiv of 1,4-butanediol are added (Fig. 11), rapid exchange occurs and a new equilibrium position is established almost immediately. Analysis of the reaction mixture by MALDI-TOF mass spectrometry and ^{11}B NMR reveals the presence of compound **22** (*m/z* 432, δ (^{11}B) +9.5), **24** (*m/z* 418, δ (^{11}B) +9.7) and **25** (*m/z* 446, δ (^{11}B) +9.9) in approximately equal proportions.

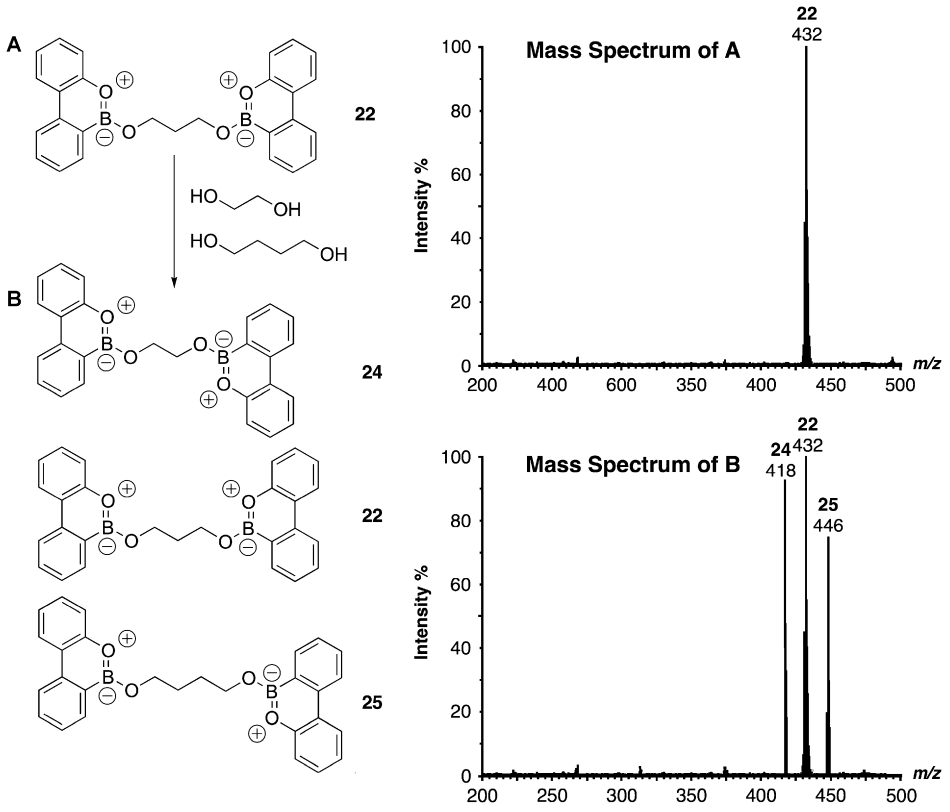

Figure 11. Treatment of a sample of **22** in acetone (mass spectrum **A**) with 1,2-ethanediol and 1,4-butanediol results in rapid re-equilibration at room temperature to give mixture of compounds **22**, **24** and **25** (mass spectrum **B**). Mass spectrum **B** was recorded 10 min after mixing the diols with compound **22**.

7. Conclusions

The formation of 1:2 adducts between **3** and a range of diols and the dynamic behaviour of these species demonstrates the utility of boroxoaromatics in dynamic covalent chemistry. The facile synthesis of compound **4** demonstrates that bifunctional boroxoaromatics required for the assembly of more complex superstructures is possible and that such compounds are stable entities, which can be handled easily. However, the lack of reactivity exhibited by **4** towards bifunctional nucleophiles in solution seriously limits its potential utility in constructing unusual or complex assemblies through dynamic selection processes. The reasons for this lack of reactivity are probably two fold. Firstly, the solubility of **4** in relatively non-polar solvents, when compared to **3**, is rather poor. This poor solubility must hamper the formation of covalent adducts by **4**. Secondly, and more importantly, placing the two boroxoaromatic rings within the same conjugated system has a detrimental effect on their reactivity. The formation of one ester by **4** will perturb the electronic structure of the system sufficiently to prevent formation of a second ester by **4**. It is therefore necessary to modify our design of bifunctional boroxoaromatics to remove the two boron containing rings from direct conjugation with each other. Such molecules are current synthetic targets in our laboratory.

8. Experimental section

8.1. General

Diethyl ether (Et_2O) and tetrahydrofuran (THF) were dried by refluxing with sodium-benzophenone under a N_2 atmosphere and collected by distillation. Toluene and xylene were distilled over sodium under N_2 and stored over 4 Å molecular sieves. Hexane and dichloromethane (CH_2Cl_2) were dried by heating under reflux over calcium hydride and distilled under N_2. All alkyllithium reagents were titrated against *N*-pivaloyl-*o*-toluidine. All other solvents and reagents were used as received. Thin-layer chromatography (TLC) was performed on aluminium plates coated with Merck Kieselgel 60 F_{254}. Developed plates were scrutinized under a UV lamp, and, where necessary, stained with iodine or PMA dip to aid identification. Column chromatography was performed using Kieselgel 60 (0.040–0.063 mm mesh, Merck 9385). Microanalyses (CHN) were carried out at the University of St. Andrews. Infra-red spectra were recorded on a Perkin Elmer 1605 FTIR spectrometer, using samples prepared as KBr discs or as thin films.

8.2. NMR spectroscopy

^1H nuclear magnetic resonance (NMR) spectra were recorded on a Bruker Avance 300 (300.1 MHz), Varian Gemini 2000 (300.0 MHz) or Varian UNITYplus (500.1 MHz) spectrometer using the deuterated solvent as the lock and the residual solvent as the internal reference in all cases. ^{13}C NMR spectra using the PENDANT sequence were recorded on a Bruker Avance 300 (75.5 MHz) spectrometer or on a Varian Gemini 2000 (75.5 MHz) spectrometer using broadband ^1H decoupling. ^{11}B NMR spectra were recorded on a Varian UNITYplus (160.4 MHz) spectrometer using the deuterated solvent as the lock and trimethyl borate as the external reference. All coupling constants are quoted to the nearest 0.1 Hz.

8.3. Mass spectrometry

Electron impact mass spectrometry (EIMS) and high-resolution mass spectrometry (HRMS) were carried out on either a VG PROSPEC or a VG AUTOSPEC mass spectrometer. Electrospray mass spectrometry (ESMS) was recorded on a VG PLATFORM mass spectrometer. Matrix assisted laser desorption ionization time-of-flight (MALDI-TOF) spectra were recorded on either a Kratos Kompact Maldi III or a Micromass Tof Spec 2E spectrometer. A nitrogen laser (337 nm, 85 kW peak laser power, 4 ns pulse width) was used to desorb the sample ions. The instrument was operated in positive linear time-of-flight mode, and results from 50 laser shots were signal averaged to give one spectrum. The matrix used was a suspension of cobalt in a methanol/glycerol mixture and was applied to the plate surface in 1-μL aliquots and allowed to dry before deposition of the analyte solution on to the matrix.

8.4. Thermal studies

Melting points were determined on an Electrothermal 9200 melting point apparatus and are uncorrected. All melting points are quoted to the nearest 0.5 °C. Thermogravimetric analysis (TGA) experiments (typical sample mass ca. 10 mg) were performed on a Perkin Elmer TGA 6 Thermogravimetric Analyzer, using nitrogen as the sample purge gas or a RheoTherm TG1000M+, using argon as the purge gas. Differential scanning calorimetry (DSC) experiments (typical sample mass ca. 5 mg) were carried out using a Perkin Elmer Pyris 1 Differential Scanning Calorimeter under helium purge or a Perkin Elmer DSC 7 under nitrogen purge.

8.5. Powder X-ray diffraction studies

Ambient temperature powder X-ray diffractograms were recorded on a Siemens D5000 diffractometer operating in transmission mode using Ge monochromatized Cu Kα1 radiation. The data were recorded for 2θ in the range 4 to 40° in steps $\Delta(2\theta)=0.02°$ and collection times varied. Variable temperature powder X-ray diffraction experiments were performed on a Siemens D5005 diffractometer equipped with an Auton Paar HTK 1200 heating stage.

8.6. Computational studies

All semi-empirical (AM1) and Hartree–Fock ab initio electronic structure calculations were performed using either SPARTAN (Version 5.0, Wavefunction, Inc., Irvine, CA, 1997) or Jaguar (Version 4.1, Release 53, Schrödinger, Inc., Portland, OR, 2001) on a Silicon Graphics Octane 2 workstation.

2-Iodoresorcinol **7** was prepared by a literature[27] method. All other known compounds were prepared by methods that differ significantly from those reported previously.

8.6.1. 2,6-Benzyloxy-1-iodobenzene 8. 2-Iodoresorcinol (3.5 g, 14.8 mmol), benzyl bromide (3.5 cm^3, 29.7 mmol), potassium carbonate (5.1 g, 37.1 mmol) and 18-crown-6 (0.2 g, 0.74 mmol) were stirred in dry acetone (120 cm^3), and the mixture heated under reflux for 15 h. After cooling, the solvent was removed in vacuo to yield a brown solid. The residue was taken up in CH_2Cl_2 (40 cm^3), water (30 cm^3) added, and the aqueous layer extracted with CH_2Cl_2 (3×20 cm^3). The combined organic extracts were dried ($MgSO_4$), and evaporated under reduced pressure. The crude product was purified by column chromatography (Et_2O/hexane, v/v, 2:3; $R_f=0.34$) to afford **8** (5.5 g, 89%) as yellow needles.

Found: C, 57.87; H, 3.96%. Calcd for $C_{20}H_{17}O_2I$: C, 57.71; H, 4.12%; mp: 90.2–91.7 °C; δ_H (300 MHz; $CDCl_3$) 7.43 (4H, d, $^3J=7.4$ Hz, Ar), 7.21–7.34 (6H, m, Ar), 7.07–7.17 (1H, m, Ar), 6.46 (2H, d, $^3J=8.3$ Hz, Ar) and 5.09 (4H, s, CH_2); δ_C (75.5 MHz; $CDCl_3$) 159.1 (Ar, quat), 137.1 (Ar, quat), 130.1 (Ar, *C*H), 128.9 (Ar, *C*H), 128.2 (Ar, *C*H), 127.4 (Ar, *C*H), 106.4 (Ar, *C*H), 80.2 (Ar, quat) and 71.4 (*C*H_2); *m/z* (EI) 416 (M^+, 12%), 91 (100); HRMS: Found: 416.0284; Calcd for $C_{20}H_{17}O_2I$: 416.0273.

8.6.2. 2,6-Benzyloxybiphenyl 9. *Method A*. A solution of phenyl boronic acid (90 mg, 0.72 mmol) in EtOH (2 cm^3) was added to 2,6-benzyloxy-1-iodobenzene (0.2 g, 0.48 mmol) and $Pd(PPh_3)_4$ (0.08 g, 0.072 mmol) in dry, degassed DME (20 cm^3). This addition was followed by treatment of the reaction mixture with Na_2CO_3 (0.16 g, 1.54 mmol) in water (5 cm^3). The mixture was heated under reflux for 3 h, and then allowed to cool. CH_2Cl_2 (20 cm^3) was added, and the mixture filtered through a short pad of Celite®. The filtrate was dried ($MgSO_4$) and concentrated under reduced pressure to afford a brown oil. Column chromatography (Et_2O/hexane, v/v, 2:3; $R_f=0.36$) afforded **9** (30 mg, 16%) as colourless plates.

Method B. A solution of bromobenzene (1.5 g, 9.6 mmol) in dry diethyl ether (20 cm^3) was added in small portions to magnesium turnings (0.23 g, 9.6 mmol), at such a rate so as to maintain a gentle reflux. After the addition was complete, the reaction mixture was heated under reflux for a further hour to ensure completion of the reaction. The solution of phenyl magnesium bromide was added slowly to a stirred suspension of 2,6-benzyloxybiphenyl (2.0 g, 4.8 mmol) and [Ni(dppe)Cl_2] (0.1 g, 0.19 mmol) in dry diethyl ether (20 cm^3). The mixture was heated under reflux for 5 h, and after cooling, diethyl ether (20 cm^3) and water (20 cm^3) were added. The aqueous layer was extracted with diethyl ether (3×20 cm^3), the combined organic extracts dried ($MgSO_4$) and concentrated to afford a yellow oil, which was purified by column chromatography (CH_2Cl_2/hexane, v/v, 1:2; $R_f=0.26$) to afforded **9** (0.77 g, 44%) as small colourless plates.

Found: C, 85.50; H, 5.89%. Calcd for $C_{26}H_{22}O_2$: C, 85.22; H, 6.05%; mp: 87–88 °C; δ_H (300 MHz; $CDCl_3$) 7.42–7.51 (4H, m, Ar), 7.22–7.38 (12H, m, Ar), 6.73 (2H, d, $^3J=8.3$ Hz, Ar) and 5.05 (4H, s, CH_2); δ_C (75.5 MHz; $CDCl_3$) 157.2 (Ar, quat), 137.8 (Ar, quat), 135.1 (Ar, quat), 131.5 (Ar, *C*H), 129.0 (Ar, *C*H), 128.7 (Ar, *C*H), 127.9 (Ar, *C*H), 127.8 (Ar, *C*H), 127.2 (Ar, *C*H), 127.0 (Ar, *C*H), 123.0 (Ar, quat), 107.2 (Ar, *C*H) and 70.9 (*C*H_2); *m/z* (EI) 366 (M^+, 21%), 91 (100); HRMS: Found: 366.1629; Calcd for $C_{26}H_{22}O_2$: 366.1620.

8.6.3. 2,6-Dimethoxyiodobenzene 11. *tert*-Butyllithium in hexanes (10 cm^3, 20 mmol, 1.2 mol equiv) was added

dropwise to a stirred solution of 1,3-dimethoxybenzene (2.5 g, 18 mmol) in THF (75 cm^3) under N_2 at 0 °C and the mixture was stirred at this temperature for a further 30 min. A solution of I_2 (4.6 g, 18 mmol) in THF (30 cm^3) was added dropwise whilst maintaining the temperature of the mixture at 0 °C. The mixture was then allowed to warm to room temperature. After 2 h, ethyl acetate (20 cm^3) was added and the mixture washed with sodium sulfite solution (2×40 cm^3, saturated aqueous solution). The organic extract was washed with aqueous NaCl solution, dried ($MgSO_4$) and concentrated under reduced pressure to afford a pale yellow solid. Recrystallization ($CHCl_3$/hexane) afforded 2,6-dimethoxyiodobenzene (3.0 g, 63%) as colourless plates.

Found: C, 36.52; H, 3.36%. Calcd for $C_8H_9IO_2$: C, 36.39; H, 3.44%; mp: 103.2–104.7 °C (lit.[28] mp: 99–100 °C); IR ν_{max} (cm^{-1}) 2840 m (OMe); δ_H (300 MHz; $CDCl_3$) 7.26 (1H, t, ^3J=8.1 Hz, Ar), 6.50 (2H, d, ^3J=8.1 Hz, Ar) and 3.88 (6H, s); δ_C (75.5 MHz; $CDCl_3$) 159.5 (Ar, quat), 129.8 (Ar, *C*H), 104.1 (Ar, *C*H), 77.6 (Ar, quat) and 56.5 (OMe, *C*H_3); *m*/*z* (EI) 264 (M^+, 100%), 249 (10), 234 (5), 221 (50) and 206 (15); HRMS: Found: 263.9652; Calcd for $C_8H_9O_2I$: 263.9647.

8.6.4. 2,6-Dimethoxybiphenyl 12. Bromobenzene (1.6 g, 10.2 mmol) in dry diethyl ether (20 cm^3) was added in small portions to magnesium turnings (0.3 g, 12.3 mmol) under N_2, at such a rate so as to maintain a gentle reflux. After addition was complete, the mixture was stirred under reflux for a further hour to ensure complete reaction. The ethereal solution of phenylmagnesium bromide was allowed to cool before it was added dropwise to a stirred solution of 2,6-dimethoxyiodobenzene (1.3 g, 4.92 mmol) and [$Ni(PPh_3)_2Cl_2$] (64 mg, 2 mol %) in dry diethyl ether (20 cm^3) under N_2. The resulting black mixture was stirred under reflux for 24 h. After cooling, water (50 cm^3) was added, and the aqueous layer extracted with ether (2×20 cm^3). Combined organic extracts were dried ($MgSO_4$) and evaporated under reduced pressure. Column chromatography (Et_2O/hexane, v/v, 1:4; R_f=0.33) afforded 2,6-dimethoxybiphenyl (0.8 g, 76%) as small colourless prisms.

Found: C, 78.34; H, 6.64%. Calcd for $C_{14}H_{14}O_2$: C, 78.48; H, 6.59%; mp: 87.0–88.1 °C (lit.[29] mp: 83–85 °C); IR ν_{max} (cm^{-1}) 2838 m (OMe); δ_H (300 MHz; $CDCl_3$) 7.48–7.29 (6H, m, Ar), 6.69 (2H, d, ^3J=8.5 Hz, Ar) and 3.76 (6H, s, Me); δ_C (75.5 MHz; $CDCl_3$) 157.9 (Ar, quat), 134.4 (Ar, quat), 131.1 (Ar, *C*H), 128.9 (Ar, *C*H), 127.9 (Ar, *C*H), 127.0 (Ar, *C*H), 119.7 (Ar, quat), 104.4 (Ar, *C*H) and 56.1 (OMe, *C*H_3); *m*/*z* (EI) 214 (M^+, 100%), 199 (16), 184 (24) and 128 (18).

8.6.5. 2,6-Dihydroxybiphenyl 5. A solution of 2,6-dimethoxybiphenyl (0.8 g, 3.7 mmol) was stirred in dry CH_2Cl_2 (20 cm^3) at −78 °C under N_2. Boron tribromide (1 M solution in CH_2Cl_2, 7.5 cm^3, 7.5 mmol) was added dropwise via a syringe and the mixture allowed to warm slowly to room temperature. After re-cooling to 0 °C, MeOH (10 cm^3) was added dropwise to quench any remaining BBr_3, and the solvents were removed on a water aspirator. Water (20 cm^3) and CH_2Cl_2 (20 cm^3) were added to the residue and the aqueous layer was extracted with CH_2Cl_2 (3×20 cm^3). Combined organic extracts were washed with water, dried ($MgSO_4$) and evaporated to dryness to afford a pale brown powder. Flash column chromatography (CH_2Cl_2; R_f=0.41) gave **5** (620 mg, 89%) as small colourless needles.

Found: C, 77.23; H, 5.34%. Calcd for $C_{12}H_{10}O_2$: C, 77.40; H, 5.41%; mp: 116–118 °C (lit.[30] mp: 118–119 °C); IR ν_{max} (cm^{-1}) 3402br (OH); δ_H (300 MHz; $CDCl_3$) 7.54–7.59 (2H, m, Ar), 7.40–7.49 (3H, m, Ar), 7.15 (1H, t, ^3J=8.1 Hz, Ar), 6.58 (2H, d, ^3J=8.1 Hz, Ar) and 4.91 (2H, br s, OH); δ_C (75.5 MHz; $CDCl_3$) 153.4 (Ar, quat), 131.0 (Ar, *C*H), 130.8 (Ar, quat), 130.2 (Ar, *C*H), 129.6 (Ar, *C*H), 129.2 (Ar, *C*H), 115.5 (Ar, quat) and 107.8 (Ar, *C*H); *m*/*z* (EI) 186 (M^+, 100%), 168 (15) and 139 (12); HRMS: Found: 186.0688; Calcd for $C_{12}H_{10}O_2$: 186.0681.

8.6.6. 5,9-Dihydroxy-5,9-dibora-4,10-dioxopyrene 4. Dichloroborane–dimethylsulfide complex (0.5 cm^3, 4 mmol) was added in small portions to a cooled, stirred solution of boron trichloride in hexane (1 M, 4 cm^3, 4 mmol). A white precipitate ($BCl_3 \cdot Me_2S$) formed immediately upon addition. The mixture was stirred with cooling for a further 10 min, and then allowed to warm to room temperature and stirred for 1 h. The resulting solution of $BHCl_2$ in hexane was added dropwise to a stirred solution of 2,6-dihydroxybiphenyl (0.3 g, 1.6 mmol) in dry toluene (20 cm^3) at room temperature. After stirring at room temperature for 2 h, $AlCl_3$ (90 mg, 0.6 mmol) was added and the mixture heated under reflux overnight. After cooling, water (20 cm^3) was added carefully, and the aqueous layer extracted with diethyl ether (3×20 cm^3). Combined organic extracts were dried ($MgSO_4$) and concentrated under vacuum to afford a pale brown solid. Recrystallization (CH_2Cl_2/hexane or acetonitrile) afforded **4** (330 mg, 87%) as small colourless prisms.

Found: C, 60.44; H, 3.47%. Calcd for $C_{12}H_8B_2O_4$: C, 60.61; H, 3.39%; mp: >400 °C (decomp.); IR ν_{max} (cm^{-1}) 3350br (OH), 1370s (OB); δ_H (300 MHz; $(CD_3)_2CO$) 8.45 (2H, s, OH), 8.39 (2H, d, ^3J=7.4 Hz, Ar), 7.68 (1H, t, ^3J=7.4 Hz, Ar), 7.43 (1H, t, ^3J=8.2 Hz, Ar) and 7.04 (2H, d, ^3J=8.2 Hz, Ar); δ_C (75.5 MHz; $(CD_3)_2CO$) 152.9 (Ar, quat), 145.3 (Ar, quat), 138.0 (Ar, *C*H), 130.1 (Ar, *C*H), 128.0 (Ar, *C*H) and 113.0 (Ar, *C*H); *m*/*z* (EI) 238 (M^+, 100); HRMS: Found: 238.0816; Calcd for $C_{12}H_8B_2O_4$: 238.0838.

Acknowledgements

We thank the Engineering and Physical Science Research Council and the University of St Andrews for financial support of this work.

References and notes

1. (a) Greig, L. M.; Philp, D. *Chem. Soc. Rev.* **2001**, *30*, 287–302; (b) Philp, D.; Stoddart, J. F. *Angew. Chem., Int. Ed.* **1996**, *35*, 1155–1196; (c) Lawrence, D. S.; Jiang, T.; Levett, M. *Chem. Rev.* **1995**, *95*, 2229–2260; (d) Lindsey, J. S. *New J. Chem.* **1991**, *15*, 153–180; (e) Whitesides, G. M.; Mathias, J. P.; Seto, C. T. *Science* **1991**, *254*, 1312–1319.
2. (a) Jahn, T. R.; Radford, S. E. *FEBS J.* **2005**, *272*, 5962–5970; (b) Gruebele, M. *Comptes. Rend. Biol.* **2005**, *328*, 701–712; (c) Kumar, T. K. S.; Yu, C. *Acc. Chem. Res.* **2004**, *37*, 929–936.

3. Klug, A. *Angew. Chem., Int. Ed. Engl.* **1983**, *22*, 565–582.
4. Stryer, L. *Biochemistry*, 3rd ed.; W. H. Freeman: New York, NY, 1988; pp 852–853.
5. For some recent examples, see: (a) MacLachlan, M. J. *Pure Appl. Chem.* **2006**, *78*, 873–888; (b) Kotch, F. W.; Raines, R. T. *Proc. Natl. Acad. Sci. U.S.A.* **2006**, *103*, 3028–3033; (c) Mancin, F.; Rampazzo; Tecilla, P.; Tonellato, U. *Chem.—Eur. J.* **2006**, *12*, 1844–1854; (d) Zeckert, K.; Hamacek, J.; Senegas, J. M.; Dalla-Favera, N.; Floquet, S.; Bernardinelli, G.; Piguet, C. *Angew. Chem., Int. Ed.* **2006**, *44*, 7954–7958; (e) Melkko, S.; Sobek, J.; Guarda, G.; Scheuermann, J.; Dumelin, C. E.; Neri, D. *Chimia* **2005**, *59*, 798–802; (f) Hahn, U.; Gonzalez, J. J.; Huerta, E.; Segura, M.; Eckert, J. F.; Cardinali, F.; de Mendoza, J.; Nierengarten, J. F. *Chem.—Eur. J.* **2005**, *11*, 6666–6672; (g) ten Cate, M. G. J.; Reinhoudt, D. N.; Crego-Calama, M. *J. Org. Chem.* **2005**, *70*, 8443–8453; (h) Schmittel, M.; Kalsani, V. *Top. Curr. Chem.* **2005**, *245*, 1–53; (i) Stoddart, J. F. *Pure Appl. Chem.* **2005**, *77*, 1089–1106; (j) Beck, J. B.; Ineman, J. M.; Rowan, S. J. *Macromolecules* **2005**, *38*, 5060–5068; (k) Keizer, H. M.; Sijbesma, R. P. *Chem. Soc. Rev.* **2005**, *34*, 226–234; (l) Piguet, C.; Borkovec, M.; Hamacek, J.; Zeckert, K. *Coord. Chem. Rev.* **2005**, *249*, 705–726.
6. (a) Zafar, A.; Hamilton, A. D. *Current Challenges in Large Supramolecular Assemblies*; Tsoucaris, G., Ed.; Kluwer Academic: London, 1999; pp 67–81; (b) Yang, J.; Marendaz, J.-L.; Geib, S. J.; Hamilton, A. D. *Tetrahedron Lett.* **1994**, *35*, 3665–3668; (c) Seto, C. T.; Whitesides, G. M. *J. Am. Chem. Soc.* **1993**, *115*, 905–916; (d) Garcia-Tellado, F.; Geib, S. J.; Goswami, S.; Hamilton, A. D. *J. Am. Chem. Soc.* **1991**, *113*, 9265–9269; (e) Lehn, J.-M.; Mascal, M.; DeCian, A.; Fisher, J. *J. Chem. Soc., Chem. Commun.* **1990**, 479–480.
7. (a) Smith, V. C. M.; Lehn, J.-M. *Chem. Commun.* **1996**, 2733–2734; (b) Stang, P. J.; Chen, K.; Arif, A. M. *J. Am. Chem. Soc.* **1995**, *117*, 8793–8797; (c) Krämer, R.; Lehn, J.-M.; Marquis-Rigault, A. *Proc. Natl. Acad. Sci. U.S.A.* **1993**, *90*, 5394–5398; (d) Hutin, M.; Frantz, R.; Nitschke, J. R. *Chem.—Eur. J.* **2006**, *12*, 4077–4082; (e) Hutin, M.; Schalley, C. A.; Bernardinelli, G.; Nitschke, J. R. *Chem.—Eur. J.* **2006**, *12*, 4069–4076; (f) Nitschke, J. R.; Schultz, D.; Bernardinelli, G.; Gérard, D. *J. Am. Chem. Soc.* **2004**, *126*, 16538–16543; (g) Schultz, D.; Nitschke, J. R. *Angew. Chem., Int. Ed.* **2006**, *45*, 2453–2456.
8. Rowan, S. J.; Cantrill, S. J.; Cousins, G. R. L.; Sanders, J. K. M.; Stoddart, J. F. *Angew. Chem., Int. Ed.* **2002**, *41*, 898–952.
9. Tam-Chang, S.-W.; Stehouwer, J. S.; Hao, J. *J. Org. Chem.* **1999**, *64*, 334–335.
10. James, T. D.; Samankumara Sandanayake, K. R. A.; Shinkai, S. *Angew. Chem., Int. Ed.* **1996**, *35*, 1911–1922.
11. (a) Rowan, S. J.; Brady, P. A.; Sanders, J. K. M. *Angew. Chem., Int. Ed.* **1996**, *35*, 2143–2145; (b) Rowan, S. J.; Brady, P. A.; Sanders, J. K. M. *Tetrahedron Lett.* **1996**, *37*, 6013–6016; (c) Brady, P. A.; Sanders, J. K. M. *Chem. Soc. Rev.* **1997**, *26*, 327–336; (d) Rowan, S. J.; Hamilton, D. G.; Brady, P. A.; Sanders, J. K. M. *J. Am. Chem. Soc.* **1997**, *119*, 2578–2579; (e) Rowan, S. J.; Sanders, J. K. M. *Chem. Commun.* **1997**, 1407–1408; (f) Rowan, S. J.; Sanders, J. K. M. *J. Org. Chem.* **1998**, *63*, 1536–1546.
12. (a) Ercolani, G.; Mandolini, L.; Mencarelli, P.; Roelens, S. *J. Am. Chem. Soc.* **1993**, *115*, 3901–3908; (b) Ercolani, G. *J. Phys. Chem. B* **1998**, *102*, 5699–5703.
13. The first definition of the term predisposition can be found in: *Comprehensive Supramolecular Chemistry*; Atwood, J. L., Davies, J. E. D., MacNicol, D. D., Vögtle, F., Eds.; Elsevier: New York, NY, 1996; Vol. 9, p 218. Sanders defines (Ref. 11d) the term predisposition as a strong conformational or structural preference expressed by the building block once incorporated into a larger structure.
14. (a) Ipaktschi, J.; Hosseinzadeh, R.; Schlaf, P. *Angew. Chem., Int. Ed.* **1999**, *38*, 1658–1660; (b) Ipaktschi, J.; Hosseinzadeh, R.; Schlaf, P.; Dreiseidler, E.; Goddard, R. *Helv. Chim. Acta* **1998**, *81*, 1821–1834.
15. (a) Cantrill, S. J.; Chichak, K. S.; Peters, A. J.; Stoddart, J. F. *Acc. Chem. Res.* **2005**, *38*, 1–9; (b) Chichak, K. S.; Cantrill, S. J.; Pease, A. R.; Chiu, S. H.; Cave, G. M. W.; Atwood, J. L.; Stoddart, J. F. *Science* **2004**, *304*, 1308–1312.
16. (a) Saur, I.; Scopelliti, R.; Severin, K. *Chem.—Eur. J.* **2006**, *12*, 1058–1066; (b) Buryak, A.; Severin, K. *Angew. Chem., Int. Ed.* **2005**, *44*, 7935–7938; (c) Saur, I.; Severin, K. *Chem. Commun.* **2005**, 1371–1473; (d) Christinat, N.; Scopelliti, R.; Severin, K. *Chem. Commun.* **2004**, 1158–1159; (e) Severin, K. *Chem.—Eur. J.* **2004**, *10*, 2565–2580; (f) Vial, L.; Sanders, J. K. M.; Otto, S. *New J. Chem.* **2005**, *29*, 1001–1003; (g) Corbett, P. T.; Sanders, J. K. M.; Otto, S. *J. Am. Chem. Soc.* **2005**, *127*, 9390–9392; (h) Corbett, P. T.; Tong, L. H.; Sanders, J. K. M.; Otto, S. *J. Am. Chem. Soc.* **2005**, *127*, 8902–8903; (i) Leclaire, L.; Vial, L.; Otto, S.; Sanders, J. K. M. *Chem. Commun.* **2005**, 1959–1961.
17. Comina, P. J.; Philp, D.; Kariuki, B. M.; Harris, K. D. M. *Chem. Commun.* **1999**, 2279–2280.
18. (a) Harris, K. D. M.; Kariuki, B. M.; Lambropoulos, C.; Philp, D.; Robinson, J. M. A. *Tetrahedron* **1997**, *53*, 8599–8612; (b) Robinson, J. M. A.; Kariuki, B. M.; Philp, D.; Harris, K. D. M. *Tetrahedron Lett.* **1997**, *38*, 6281–6284.
19. Robinson, J. M. A.; Philp, D.; Kariuki, B. M.; Harris, K. D. M. *J. Chem. Soc., Perkin Trans. 2* **2001**, 2166–2173.
20. Greig, L. M.; Kariuki, B. M.; Habershon, S.; Spencer, N.; Johnston, R. L.; Harris, K. D. M.; Philp, D. *New J. Chem.* **2002**, 701–710.
21. Stanforth, S. P. *Tetrahedron* **1998**, *54*, 263–303.
22. Thomsen, I.; Torssell, K. B. G. *Acta Chem. Scand.* **1991**, *45*, 539–542.
23. Banzatti, C.; Carfagna, N.; Commisso, R.; Heidempergher, F.; Pegrassi, L.; Melloni, P. *J. Med. Chem.* **1988**, *31*, 1466–1471.
24. X-ray diffraction studies on crystals of **4**, grown by slow evaporation of an acetonitrile solution, were performed using a Bruker SMART/Mo system. The structure was solved by direct methods, the non-hydrogen atoms were refined (Ref. 31) with anisotropic displacement parameters, hydrogen atoms bound to carbon were idealized and fixed (C–H 0.95 Å). Crystal data for **4**; $C_{12}H_8B_2O_4$, colourless prism, 0.18×0.1×0.1 mm, M=237.80, tetragonal, a=32.1413(9) b=32.1413(9) c=4.0964(2) Å, α=90 β=90 γ=90°, F(000)=1952, U=4231.8(3) Å^3, T=293(2) K, space group $I4_1/a$, Z=16, μ(Mo Kα)=0.108 mm^{-1}, $2\theta_{max}$=46.54°. Of 1527 measured data, 994 were unique reflections (R_{int} 0.0391) to give $R1$ [$I>2\sigma(I)$]=0.0327 and $wR2$=0.1018. Crystallographic data (excluding structure factors) have been deposited with the Cambridge Crystallographic Data Centre as supplementary publication no. CCDC 607600. Copies of the data can be obtained free of charge on application to CCDC, 12 Union Road, Cambridge CB2 1EZ, UK [fax: +44 1223 336 033; e-mail: deposit@ccdc.cam.ac.uk].

25. A related bis-boroxoaromatic compound, 5,12-dihydroxy-5,12-dibora-6,13-dioxodibenz[*a*,*h*]anthracene, has been reported as showing similar behaviour. Unfortunately, no structural details were provided: Offenhauer, R. D.; Rodewald, P. G. *J. Polym. Sci., Part B* **1968**, *6*, 573.
26. X-ray diffraction studies on crystals of **22**, grown by slow evaporation of an acetonitrile solution, were performed using a Bruker SMART/Mo system. The structure was solved by direct methods, the non-hydrogen atoms were refined (Ref. 31) with anisotropic displacement parameters, hydrogen atoms bound to carbon were idealized and fixed (C–H 0.95 Å). Crystal data for **22**; $C_{27}H_{22}B_2O_4$, colourless prism, 0.14×0.1×0.1 mm, M=432.07, monoclinic, a=19.301(3) b=5.2214(7) c=22.837(3) Å, α=90 β=107.316(4) γ=90°, F(000)=904, U=2197.2(5) Å^3, T=293(2) K, space group $P2_1/c$, Z=4, μ(Mo Kα)=0.085 mm^{-1}, $2\theta_{max}$=46.58°. Of 3103 measured data, 1414 were unique reflections (R_{int} 0.0439) to give $R1$ [$I>2\sigma(I)$]=0.1345 and $wR2$=0.4164. Crystallographic data (excluding structure factors) have been deposited with the Cambridge Crystallographic Data Centre as supplementary publication no. CCDC 607601. Copies of the data can be obtained free of charge on application to CCDC, 12 Union Road, Cambridge CB2 1EZ, UK [fax: +44 1223 336 033; e-mail: deposit@ccdc.cam.ac.uk].
27. Weitl, F. L. *J. Org. Chem.* **1976**, *41*, 2044–2045.
28. Anderson, J. C.; Pearson, D. J. *J. Chem. Soc., Perkin Trans. 1* **1998**, 2023–2029.
29. Saa, J. M.; Martorell, G.; Garcia-Raso, A. *J. Org. Chem.* **1992**, *57*, 678–685.
30. Joschek, H.-I.; Miller, S. I. *J. Am. Chem. Soc.* **1966**, *88*, 3269–3272.
31. Sheldrick, G. M. *SHELXTL, version 6.10, Program for Crystal Structure Solution*; Bruker AXS: Madison, WI, 2002.